JOURNAL OF NANO- AND ELECTRONIC PHYSICS
Vol. **7** No 4, 04016(7pp) (2015)

ЖУРНАЛ НАНО- ТА ЕЛЕКТРОННОЇ ФІЗИКИ
Том **7** № 4, 04016(7cc) (2015)

Behavior of Zr1 %Nb Alloy Under Swift Kr Ion and Intense Electron Irradiation

V.F. Klepikov[1], V.V. Lytvynenko[1], Yu.F. Lonin[2], A.G. Ponomarev[2], O.A. Startsev[1,*], V.T. Uvarov[2]

[1] *Institute of Electrophysics and Radiation Technologies, NAS of Ukraine, 28, Chernyshevsky Str., PO 8812, 61002 Kharkiv, Ukraine*
[2] *NSC Kharkiv Institute of Physics and Technology, NAS of Ukraine, 1, Akademichna Str., 61108 Kharkiv, Ukraine*

(Received 19 August 2015; revised manuscript received 04 December 2015; published online 10 December 2015)

In this paper there were studied the physical and mechanical properties of Zr1 % Nb alloy irradiated by the Kr ion beam with energy of 107 MeV, fluences of $1 \cdot 10^{13}$ and 10^{14} ion/cm^2, and exposed to the microsecond high-current pulsed electron beam with the energy of 370 keV, incident energy fluence in the range of 20…200 J/cm^2. The low-intense Kr ion implantation induced softening of the alloy. The high-intense ion beam irradiation resulted in creation of a surface strengthened layer with nanohardness of 4.5 GPa and the elastic modulus of 120 GPa. The high-current electron beam exposure lead to the macroscopic surface melting of the sample, which provoked formation of the coarse structure with predominantly brittle fracture character.

Keywords: Zirconium, Electron beam, Swift heavy ions, Ablation.

PACS numbers: .61.80.Fe, 61.82.Bg, 81.40.Wx

1. INTRODUCTION

The main design components of the heterogeneous active zone of nuclear reactor are the fuel roads, moderator and coolant, which types determine the total financial expenses for building and further exploitation of all nuclear facility. Besides the current progress on developing novel nuclear reactors [1], research on more efficient nuclear materials for existing reactors, which will provide higher core temperature along with operation cycle, has never been stopped. Especially nowadays, when our world faces a new challenge for cheap energy resources and best sell markets.

The technical requirements for the fuel roads are very rigorous in order to guarantee the safety of nuclear facility. In a long list of them, we should distinguish the construction simplicity, mechanical strength under minimal presence of construction materials in active zone, resistance to coolant and nuclear fuel as well as small neutron absorption cross-section.

Zirconium and its alloys are common materials for the fuel roads for PWR, WWER reactors [2]. Zirconium has the relatively low absorption cross-section of thermal neutrons of around 0.18 barn, melting temperature is slightly higher than 1800 °C, initiation temperature (vapor-gas reaction) of hydrogen generation is around 861 °C, which provide a high margin of thermal safety for the fuel rods and nuclear fuel under critical, emergency conditions. The modernized Zirconium alloys should have higher corrosion resistance and lower absorption of hydrogen. Good corrosion resistance to coolant and fuel provides the construction integrity, low absorption of hydrogen slow down the embrittlement of Zirconium, which is critical to avoid the crack generation and macroscopic deformation as well. The advanced nuclear materials for tubes are necessary to increase the effective power of the nuclear power plants (NPP), prolongation of the exploitation cycle, more effective burning of the fuel (e.g., increasing the fuel burning to 70 (MW·day)/(kg U), exploitation duration of the fuel up to 7 years for WWER-1000) [3].

During exploitation of PWR, WWER reactors, the fuel-rod cladding tubes degrade under the different factors such as: bombardment of the internal tube surface by the decay fragments, swelling of nuclear fuel due to accumulation of the solid and gaseous fission products, gassing of fission products from the fuel bulk beneath the internal surface of tubes. The typical decay rate is around 1.3 decay/(cm^3·s), each decay of ^{235}U produces fission fragments with masses distributed around 95 a.m.u. and 135 a.m.u. Their kinetic energy is enough to pass in Zirconium up to 10 μm. It is worth noting, that the flux of high-energy decay fragments is around $5 \cdot 10^9$ ion/(cm^2·s), and affects on the inner surface of tubes, which induces the formation of ion-implanted layer [4].

Among all the fission products in the thermal neutron reactors, the noble gases Xe and Kr are very important. These fission fragments have two special properties – very low dissolution and preferably gaseous state. In addition, these gases are trying either to extract from the fuel matrix and accumulate in free space of the fuel rods, when it is kinetically possible, or to generate certain clusters inside the fuel, which results to formation of the gaseous bubbles. Thus, these difficulties leading to the need for assessment of influence of the gaseous products on the tubes, and that could be done via exposure by ion beams, especially swift heavy ions (SHI) [5, 6].

In literature, there are some related results focused on investigation of Zirconium and Zr-Nb-alloys under the ion exposures [5, 7, 8]. For instance, in [5] it was found, that the ion irradiation (^{4}He^{+1} and ^{40}Ar^{+1}, energy ~ 2..4 keV, effective beam current ~ 1 mA/cm^2, fluence ~ $2..4 \cdot 10^{18}$ ion/cm^2, target temperature ~ 150 °C, pressure ~ 10^{-6} Pa) of E110, E625 Zirconium alloys improves their mechanical properties. The authors noticed the significant increase of wear resistance and microhardness due to the structural homogenization in the modified shallow surface layer.

* startsev-alex@ukr.net

The available experimental results [5, 7] represents research on modification of Zirconium alloys by the low-energy ion beams (< 1 MeV/nucleon) in the different intensity ranges, however, it is necessary to reveal Zr1 % Nb alloy properties under heavy ion exposure in the energy range of about 1 MeV/nucleon, which is specific to gaseous fission products like Xe and Kr.

Regarding incidents on Fukushima Daiichi, it is of great importance to investigate the response of alloy to the intense energy loads. The possible technique to test material's properties is the high-current electron beam (HCEB) [9-11]. In fact, HCEB enables to test material properties under extreme thermal and shock conditions, which could happen in the active zone during emergencies at NPPs.

In [9] the Zr1 % Nb alloy was processed using the pulsed HCEB with the energy of 18 keV, density ~ 19 J/cm^2, impulse duration of 50 μs. That treatment increased the hardness and wear resistance in the 8-μm near-surface layer by 40 % and 30 %, respectively. The thin martensitic layer was also formed with a thickness of 2 μm, which effectively prohibit the hydrogen diffusion. This layer has good gas-barrier properties due to 3-fold reduction of hydrogen sorption into the material bulk.

Dovbnya et al. in [3] investigated the modification of Zr1 % Nb by the HCEB with the energy in the interval of 70…80 keV, density ~ 10...20 J/cm^2, impulse duration of 15 μs, frequency ~ 2 Hz, 5 impulses total. After irradiation, the nanostructured surface layer had the improved nanohardness to 3.8 GPa, compared to the initial nanohardness of 2.3 GPa. This strengthening effect was induced by the phase transitions, which occurred during fast cooling (up to 10^8 K/s) with formation of the plate-like metastable phase in the alloy microstructure. The mentioned phase generated high internal stresses, which resulted in the hardness enhancement.

Nonetheless, we only found the literature results on the e-beam exposure either by the high-current low-energy pulses (~ 1 kA, < 100 keV) or low-current relativistic steady pulses (~ 50 mA, ~ 1 MeV) with the energy density up to 30 J/cm^2. The experimental data about the intense e-beam damage in intense ablation mode (> 50 J/cm^2) of Zirconium is still lacking.

In this paper, we apply the microsecond intense HCEB irradiation at the TEMP-A accelerator [12]. The microsecond timescale provides its own advantages over nanosecond or sub-second exposure. The lifetimes of phase instabilities induced in target medium by the microsecond HCEB are approximately equal several microseconds. Moreover, some metastable phases could be 'frozen' by fast cooling (up to 10^9 K/s) through thermoconductance into the bulk and radioconductance at the hot surface. While the high-speed cooling limits the equalizing diffusion processes, even longer e-beams impulses (~ 1 ms) could result in significant modification.

The theoretical and numerical background on simulation of radiation damage in the nuclear materials by fission products and SHI beams is quite solid (e.g., SRIM / TRIM) [7], although it needs experimental assessment. For intense relativistic e-beam damage of metals with electron energy in the interval of 0.200…4 MeV, energy density of 10…500 J/cm^2, when the heat source has explicit volumetric character and damage products are liquid, gaseous, plasma and solid fragments, it is not convenient to use certain mathematical or numerical model due to the different physical approaches and great amount of fitting coefficients. For very intense sub-microsecond pulses (~10^{13} W/cm^2), the most useful is the hydrodynamic model proposed in 1981 by Romanov and Suzdenkov [10]. The dislocation-based models for nanosecond e-beam exposures (≤ 10^8 W/cm^2, ≤ 50 J/cm^2) were developed by Mayer et al [11], which allow to simulate the plastic deformation of targets, estimate the temperature dynamics, stress evolution, and generation of plasma cloud.

In [13-15] we presented our attempts on simulation of HCEB modification of metals. It was developed in [13] a simple semi-empiric thermal model of e-beam ablation based on the hyperbolic Maxwell-Cattaneo-Lykov law for the heat conductance, Stefan problem and the weakly coupled dynamic theory of thermoelasticity. Its elastic part was reduced to calculation of the stress jumps on the boundaries of solid-melt fronts to simplify tracking of volumetric damage under intense e-beam heating. The stated thermal model was numerically implemented using finite difference methods and tested for the wrought Aluminum alloy 1933. The heating and cooling temperature evolution, corresponding gradients, their speeds and fronts were evaluated in the case of the homogeneous medium. After more comprehensive tests, it was found, that this model usually overestimates by 20 % the mentioned characteristics for light metals and Iron exposed at TEMP-A conditions. Thus, in [14] we specified more carefully the dynamics of temperature and displacement fields in a homogeneous target through developing the thermoelastic model of e-beam ablation within the Maxwell-Cattaneo-Lykov law modified to consider the impact of deformation on the temperature field, elastic part with the small strain tensor and body force induced by the thermal expansion. That model was numerically implemented using classical Galerkin finite element method (FEM) and tested for the Titanium alloy VT1-0. In this paper, we employed the later more proper model [14] to assess numerically the induced displacements and temperature, and compare them with experimental data.

Our research aiming to study the response of the experimental alloy Zr1 % Nb to irradiation by (i) the swift heavy ion beam and (ii) intense electron beam in the ablation mode.

2. MATERIALS AND METHODS

The samples were prepared from the fuel rod's wall of experimental alloy Zr1 % Nb, which was produced using Iodine Zirconium, melted in the arc-furnace in the inert atmosphere. The initial thickness of samples equals 0.65 mm, width and length of 3.5 mm × 10 mm, respectively. The samples for ion irradiation were previously mechanically thinned to 200 μm and electropolished in CH_3COOH + 10 % $HClO_4$ solution during 25 s under the electrode potential of 30 V.

Intense electron irradiation of Zr1 % Nb alloy was conducted under the pressure around 10^{-5} torr at the

TEMP-A high-current e-beam pulsed accelerator facility [12] with the following parameters: electron energy ~ 0.37 MeV, beam current ~ 2 kA, 5 μs beam pulse in the intensity range of 10^5…10^7 W/cm^2, one impulse applied. Energy density released on the exposed surface did not exceed 5 MJ/m^2.

Two identical samples were irradiated at the cyclic implantator of heavy ions IC-100 (FLNR, JINR, Dubna) [16] by $^{86}Kr^{15+}$ ions with the fluences of $1{\cdot}10^{13}$ and 10^{14} ion/cm^2. The incident density was 10^{10} ion·cm^{-2}s^{-1}, intensity of 2 μA, energy ~ 107 MeV, and the beam incidence angle of 30°w.r.t. the surface. The specific energy of ions (~ 1.2 MeV/nucleon) was enough to experimentally simulate the energy deposition of fission products through preferable inelastic collisions. The temperature of samples under exposure was less than 25 °C to prevent their overheating. The homogeneity of ion irradiation was achieved through vertical and horizontal beam scanning with frequencies of 100 Hz and 200 Hz, respectively. The vacuum in the irradiation chamber was around $5{\cdot}10^{-7}$ torr. The beam scanning in horizontal and vertical directions has been applied to achieve homogeneity of ion beam processing of the target surface better than 5 %.

Visual and morphological analyses of the ion- and e-beam-irradiated samples were performed using the optical microscope Bresser BioLux NV. Topographical analysis of the cross-fractures was conducted using the scanning electron microscope JEOL JSM-840. Then, the cross-sections were prepared for metallographic and hardness analyzes of the samples after both kinds of irradiation. The metallographic specimens were polished using a micron diamond powder W0-1. The hardness H_{50} of the modified near-surface zones was measured with the PMT-3 microhardness testing machine equipped with Berkovich trihedral diamond pyramid with an applied load of 50 kgf. Estimates of the elastic modulus E and nanohardness H of the samples were obtained using the continuous stiffness method on the MSSI's Agilent Nano Indenter G200 by Berkovich trihedral indenter with the tip radius of 20 nm to the indentation depth up to 500 nm with the step of 15 μm, 4 measurements in the vicinity of each point in the uniformly modified zone. H and E were measured through all the thickness of the e-beam irradiated samples. In the case of the thin ion-implanted samples, the mentioned characteristics were obtained to the indentation depth of 200 nm. To enhance the precision, the samples were placed on the special holder to stabilize the temperature 1 hour before performing the measurements themselves. The hardness was calculated using the classic Oliver-Pharr analysis method. After hardness measurements had been performed, metallographic analyses were done. To detect the microstructure of the material, the chemical etching was carried out using the reagent of 5 % HF, 15 % HNO_3 + 80 % H_2O at the room temperature around 24 °C, etching time of 4 s.

3. ZR1 %NB ALLOY AFTER KR ION IRRADIATION

Visual examination of the surfaces after the swift Kr exposures showed their erosion, especially for the fluence 10^{14} ion/cm^2 (see Fig. 1a, b). The processed surfaces have microscopic craters and hillocks. Under low fluence, the formation of craters initiates on the initial surface defects such as scratches, grain boundaries. With the increase of fluence, the irregularity of irradiation-induced defects increases.

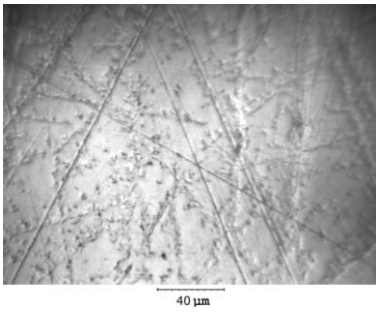

a

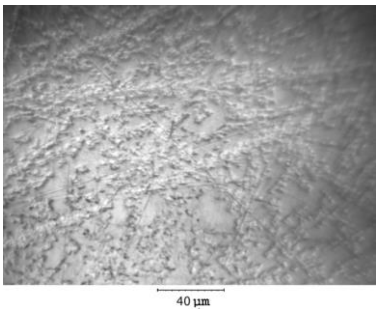

b

Fig. 1 – Surface of Zr1 % Nb alloy after irradiation by $^{86}Kr^{15+}$ ions (107 MeV) with fluence of 10^{13} ion/cm^2 (a) and 10^{14} ion/cm^2 (b)

The radiation damage induced by the SHI irradiation is not uniform in the target's bulk. In order to estimate the volumetric distribution of the radiation damage it is necessary to conduct evaluation of the defect generation profile and induced displacements using SRIM-2010 package. The total dose D (in dpa) can be determined as (1):

$$D = \sigma_d \, \Phi \,, \tag{1}$$

where σ_d is the defect generation, Φ is the fluence. σ_d is a general characteristic of materials damageability defined by (2):

$$\sigma_d = N_d^{1ion} \, M_{mol} \Big/ \rho \, d \, N_A \,, \tag{2}$$

where N_d^{1ion} is the average number of displacements provoked by one ion, M_{mol} is the medium molar mass, ρ is the medium density, d – the damage peak thickness, N_A – the Avogadro constant. For the sake of practical advantage, we could rewrite (2) to (3):

$$\sigma_d = \eta \, \Psi \, / \, N \,, \tag{3}$$

where Ψ is the rate of introduction of defects into the medium, which is measured in vac/(Å·ion), N – the concentration of atoms in a volume unit, η (10^8 Å/cm) is the dimensional coefficient, which defines the correlation between units of Ψ and N. Further, Ψ can be directly simulated in SRIM for the Zr1 % Nb alloy. We conducted calculations with the next parameters: alloy density

$\rho = 6.46$ g/cm^3 at $T = 300$ °C, the displacement energy for hcp-Zr $E_d^{Zr_{hcp}} \sim 40$ eV [17, 18]. At this temperature, 0.3 wt. % of Nb dissolves in the Zr matrix, the remainder part ~ 0.7 wt. % of Nb formes β-Nb phase with bcc lattice. Therefore, we used the displacement energy for bcc-Nb $E_d^{Nb_{bcc}} \sim 60$ eV [17]. For all calculations the lattice bond energy and the surface energy were equal to 0 eV. The SRIM calculation gave us the maximal value of $\Psi \sim 1.63$ vac/(Å·ion) at the depth of 10 μm. Finally, as follows from numerical simulations (with statistics of 10^5 events) and applying (3), we've obtained Fig. 2, which represents the defect generation profile σ_d for the Zr1 % Nb alloy at 300 °C. Applying (1), the displacements for the fluences of 10^{13} ion/cm^2 and 10^{14} ion/cm^2 are 0.076 and 0.76 dpa at the 10 μm depth, consequently.

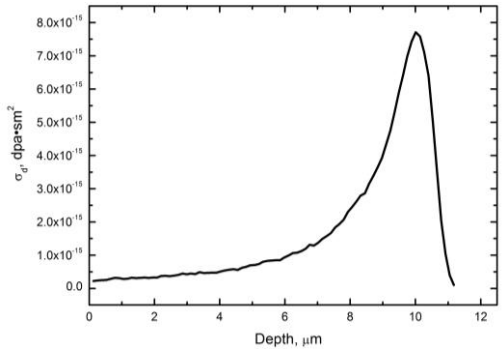

Fig. 2 – Defect generation depth profile σ_d for Zr1 % Nb alloy for Kr ion irradiation

We analyzed the nanohardness H and elastic modulus E of the Kr irradiated samples and 'as-fabricated' alloy. It was noticed the nontrivial dependence of H and E on the fluence (see Fig. 3). A slope is observed for these characteristics from the beginning to 40...50 nm, which corresponds to the elastic deformation mechanism. Worth noting, the hardness gradient is relatively the same up to the depth of 38 nm and does not depend on the processing: $\nabla H \sim 0.05$ GPa/nm. In the case of the highest fluence 10^{14} ion/cm^2, this slope transforms to local maximums of H and E in the interval of 35…60 nm, which equal to 4.9 GPa and 127 GPa, accordingly. Such peak values can be explained by presence of the surface oxide layer. After 70 nm the deformation mechanism is plastic, the curves become flattened, and the experimental data can be statistically averaged. After implantation by 10^{13} ion/cm^2 the nanohardness decreased to 3.4 GPa, in contrast to the initial value of 3.6 GPa. Neglecting small variations, elastic modulus is very close to the unirradiated material, although E shows a considerable reduction up to the depth of 55 nm compared to the unirradiated alloy. That degradation of E can supposedly be a result of some amorphization of the surface oxide layer. The softening process might be provoked by the local recovery of the radiation damage regarding high local temperatures and excitation of the electronic structure during the ion treatment, which provides enough energy for developing of the dislocation microsystem while temporary limiting the stabilization property of Nb.

In the higher dose region, the sample exhibited the significant increase in nanohardness by 25 % and averagely

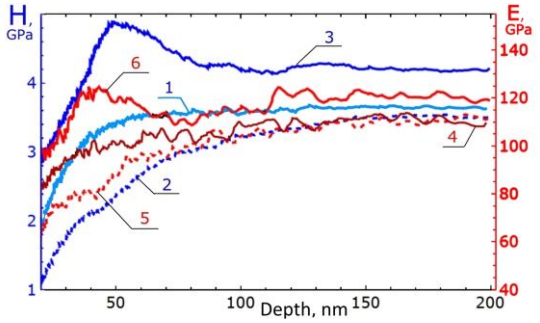

Fig. 3 – Surface nanohardness (H, blue, left axis) and elastic modulus (E, red, right axis) versus indentation depth (L): (1-3), (4-6) – plots of H and E for non-modified, irradiated with fluence of 10^{13} ion/cm^2 and 10^{14} ion/cm^2, respectively

equaled to 4.5 GPa. The elastic modulus E also became a little bit larger $E \sim 120$ GPa. The improved mechanical characteristics after Kr exposure of 10^{14} ion/cm^2 can be explained by the radiation defects and formation of metastable phases [6]. It should be noted, these results are moderate owing to the fact, that our samples have been irradiated at the room temperature. However, such low-temperature SHI implantation raises the influence of hardening [6], enabling to observe the effects occurred at higher doses, whereas the impact of softening mechanism at the real operating temperature around 300…400 °C is considerable. Thus, the observed difference in response of mechanical properties to the Kr bombardment with two fluences showed the complexity of predicting the tubes parameters for the real nuclear conditions, and proved an obvious advantage of high-energy ion testing. For further research on the specifics of transformation from radiation-enhanced softening to hardening more advanced techniques are needed.

4. INTENSE E-BEAM MODIFICATION OF ZR1 % NB ALLOY

HCEB irradiation resulted in formation of the inhomogeneous surface, which roughness significantly varies. Fig. 4 shows the surface in the epicenter of exposure (20…200 J/cm^2) and in the periphery (< 40 J/cm^2) zone. The e-beam heating provoked intense melting and evaporation of the surface. The ablated debris were ejected into the vacuum chamber and some amount was redeposited onto its surface.

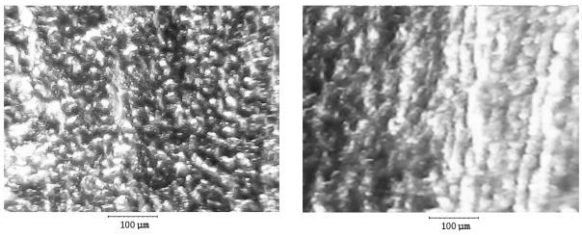

Fig. 4 – Surface morphology of Zr1 % Nb alloy after intense electron beam irradiation: (a) – epicenter, (b) – transition from epicenter (dark left side) into periphery (light right side)

Based on the optical analyses, the maximal depth of crater approximately equals 80 μm. The formed coating in the epicenter predominantly consists of the solidified

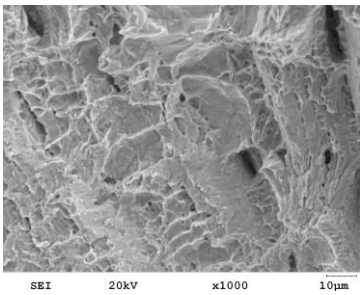

a

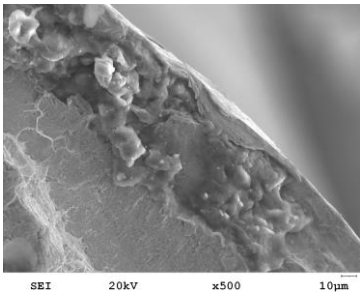

b

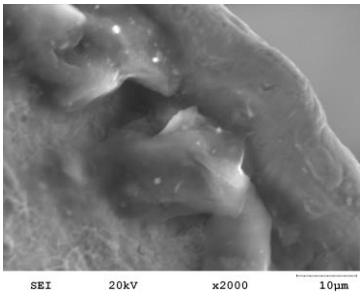

c

Fig. 5 – Fractures of Zr1 % Nb alloy: (a) – unirradiated material, (b) – epicenter of intense electron beam modification, and (c) – periphery of exposed sample

droplets with the linear size in the range of 30..50 μm without specific orientation. The periphery zone characterizes by relatively smooth surface with the periodical ridges of 10 μm height and 40 μm distance among them. The periodicity is clearly pointed perpendicularly to the centrifugal direction from the epicenter zone. The melt was ejected from the epicenter, and then the ablated products were back condensed and smoothed upon the surface in accordance to their kinetic energy.

The investigations of the cross-fractures showed, that the HCEB impact has changed the microstructure crucially. The damage mechanisms in the unirradiated and irradiated zone occurred by different way. The unmodified Zr1 % Nb alloy exhibits basically ductile fracture surface with fine ridges, small voids, large dimples with incomplete rims and small dimples with complete rims. It demonstrates the transgranular damage character (Fig. 5a). Fracture has local areas of tearing topography. We also noticed the deep chimney-like depressions elongated parallel to the surface, deformed flutes and few fracture ledges with quasi brittle character as a result of shear overloading. According to the metallographic data, the initial microstructure of the Zr1 % Nb alloy consists of the equiaxed grains with the linear size of 3…5 μm.

Further, the irradiated material has brittle type of fracture (Fig. 5b). In the heat-affected melted zone the cracks propagated along the grain boundaries. The intensively exposed material has nonuniform rough fracture surface with coarse grains and short intergranular cracks directed towards the surface or perpendicular to it. There were found shallow cavities and deep voids filled with damage debris. In contrary to the epicenter zone, the periphery shows highly compactified dense structure without cracks (Fig. 5c). The large recrystallized grains are embedded into the Zirconium matrix. The thickness of the modified zone in the epicenter and in the periphery is up to 70 μm and 30 μm, correspondingly. The recrystallized layer consists of coarse grains with the size in the range of 10…20 μm.

In addition, we found, that a 10 μm surface layer was damaged in the ductile manner in the periphery zone, after which the fracture surface changes to intergranular brittle type (Fig. 5c). Worth noting, this ductile surface layer is not an oxide layer, and it only covers the low-dose irradiated area (20…40 J/cm^2). The physical origin of formation of such thin ductile zone assumed to be rapid solidification of the vapor ejected from the epicenter, without heat supply to provoke further grain growth, unlike the material deeper in the bulk. Moreover, such structure can form only in the special areas of irradiation, when the incident e-beam provides enough heat to melt shallow surface layer but no large droplets condensing on the surface. Other areas of the periphery, where droplets condensed, have quite chaotic and rough structure with lots of intergranular cracks.

There was also found an oxide layered structure on the surface, which formed due to high residual temperature, when the sample was taken from the vacuum chamber. It has the maximal thickness of 4 μm in some defect places (e.g. it covers surface dimples, cracks) in the epicenter of exposure. We noticed signs of the decohesive rupture between the oxide layer and the melted zone. Adhesion between the basic material and heat-affected zone is relatively good, without any macrocracks.

As observed by microhardness and nanohardness measurements (Table 1), the mechanical properties markedly depend on the local energy fluence the material was subjected to. The intense irradiation degraded the modified layer in the epicenter: the microhardness H_{50} reduced by 12 %, E by 4 %, and H by 14 %, compared to the 'as-fabricated' material. Notwithstanding, the material properties in the periphery increased: H_{50} by 17 %, E by 4 %, and H by 6 %, which can be induced by fast quenching, dense structure, good adhesion to matrix and absence of cracks.

Table 1 – Mechanical properties of the Zr1 % Nb alloy before and after e-beam exposure

№	Material	H_{50}, GPa	H, GPa	E, GPa
1	Non-irradiated	2.4	3.5	113
2	Epicenter	2.1	3.0	108
3	Periphery	2.8	3.7	117

We also compared the experimental data with the numerically simulated temperature and thermal displacements dynamics in 2D space {beam width × depth of penetration} using FreeFem++v3.380001 according to our model developed in [14] (see Fig. 6a, b). The material

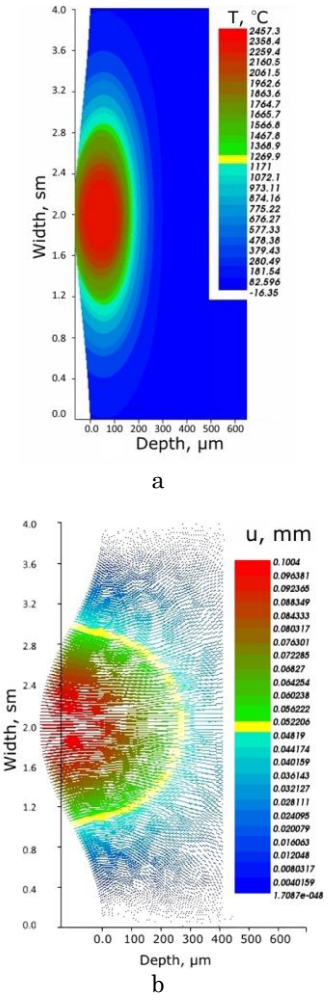

Fig. 6 – Simulated temperature (a) and displacements in Zr1 % Nb alloy after 5 μs electron beam exposure

parameters of Zr1 % Nb for the calculations were taken from [2]. In contrary to the research on Ti [14] and Al [13, 15], the calculated penetration depth of HCEB is greater than the maximal real thickness of the processed layer including crater: 80 μm + 70 μm vs. 200 μm. Such difference is a result of the real tough rigid structure and low thermal conductivity of the alloy, and we did not take into account in calculations the former one properly. Thus, the behavior of the experimental Zr1 % Nb alloy under the concentrated energy impact in the range of 20…200 J/cm^2 is quite better than expected from similar research on the lighter materials. The subsurface melting, which is typical for light alloys and stainless steels, does not prevail in these damage processes, the surface melting and evaporation predominate though. Surface ablation prevents the deeper layers from the destruction like a thermal insulator.

At the same time, the resistance to high thermal loads was found in the laboratory conditions, when Zirconium did not contact with the nuclear fuel, the heat source is only the volumetric microsecond energy deposition of certain electron beam, and the melt removes freely into the vacuum chamber. At least, as has been pointed out above, that embrittlement of Zr1 % Nb take place after accidental melting of the tube even in vacuum conditions. Interaction of the heated material with the nuclear fuel will only deteriorate the problem.

However, the HCEB modification could be useful for surface modification of Zirconium. The results indicate, if the intensity of impact is low (< 40 J/cm^2) and the material is subjected to strong cooling, a thin protective coating with compacted structure forms, which has enhanced mechanical properties. But the structural integrity and physical-mechanical properties definitely degrade after the impact with fluence above 40 J/cm^2.

5. CONCLUSIONS

We studied the tolerance of experimental Zr1 % Nb alloy upon irradiation by the swift $^{86}Kr^{15+}$ ion beam and intense electron beam exposure.

The irradiation with swift $^{86}Kr^{15+}$ ions has almost no significant influence on the elastic modulus in contrast to the nanohardness. The hardness of the Zr1 % Nb alloy has been found to be dependent on the applied fluence. After Kr exposure with the fluence of $1 \cdot 10^{13}$ ion/cm^2 the nanohardness of the surface layer reduced by 6 %, but the fluence of $1 \cdot 10^{14}$ ion/cm^2 increased the nanohardness by 25 %. The observed hardening effect and the changes of elastic modulus corresponds with the recent result presented in [6] on the Xe^{26+} ion irradiation of the Zr1 % Nb alloy. In addition, intense $^{86}Kr^{15+}$ ion impact also induced formation of the protective oxide layer at the depth of 35...60 nm with the enhanced nanohardness by 36 % and elastic modulus by 10 %.

The increase in microhardness and elastic modulus of the sample irradiated with microsecond quasirelativistic electron beam was found at the periphery zone with the fluence not more 40 J/cm^2. It may be caused by the fast quenching processes, which provoke formation of the crackless dense microstructure below the thin surface ductile layer, whilst the reduced mechanical properties of the same sample at the epicenter zone with the fluence of 30…200 J/cm^2 could be a result of grain growth, cracks generation by relaxation of residual thermal stress and oxidation. Embrittlement was detected almost for all the electron beam melted material, therefore, it can be deduced, that in any cases, the behavior of the Zr1 % Nb alloy will degrade under real accident conditions with the fluence on the rod's surface above 40 J/cm^2.

AKNOWLEDGEMENTS

Authors are grateful to the National Academy of Sciences of Ukraine for providing financial support (grant No ЦО 16-2/2015) and to Dr. V.A. Skuratov (JINR, FLNR) for irradiation of test samples by SHI beam. O.A. Startsev gratefully acknowledges the excellence scholarship awarded from the Presidium of National Academy of Sciences of Ukraine.

Поведінка сплаву Zr1 % Nb під інтенсивним електронним опроміненням і швидкими іонами Kr

В.Ф. Клепіков[1], В.В. Литвиненко[1], Ю.Ф. Лонін[2], А.Г. Пономарьов[2], О.А. Старцев[1], В.Т. Уваров[2]

[1] *Інститут електрофізики і радіаційних технологій НАН України, вул. Чернишевського, 28, 61002 Харків, Україна*
[2] *ННЦ Харківський фізико-технічний інститут НАН України, вул. Академічна, 1, 61108 Харків, Україна*

В цій роботі досліджувались фізичні і механічні властивості сплаву Zr1 % Nb опроміненого за допомогою пучка іонів Kr з енергією 107 МеВ, флюенсами $1{\cdot}10^{13}$ і 10^{14} іон/см^2, а також під впливом мікросекундного сильнострумового імпульсного пучка електронів з енергією 370 кеВ, падаючим потоком енергії в інтервалі 20…200 Дж/см^2. Низькоінтенсивна імплантація іонів Kr спричинила пом'якшення сплаву. Високоінтенсивне опромінення іонним пучком зумовило утворення поверхневого зміцненого шару з нанотвердістю 4.5 ГПа і модулем пружності 120 ГПа. Опромінення сильнострумовим електронним пучком призвело до макроскопічного поверхневого оплавлення зразку, що спричинило утворення крупнозернистої структури з переважно крихким характером зламу.

Ключові слова: Цирконій, Електронний пучок, Швидкі важкі іони, Абляція.

Поведение сплава Zr1 % Nb под интенсивным электронным облучением и быстрыми ионами Kr

В.Ф. Клепиков[1], В.В. Литвиненко[1], Ю.Ф. Лонин[2], А.Г. Пономарев[2], А.А. Старцев[1], В.Т. Уваров[2]

[1] *Институт электрофизики и радиационных технологий НАН Украины, ул. Чернышевского, 28, 61002 Харьков, Украина*
[2] *ННЦ Харьковский физико-технический институт НАН Украины, ул. Академическая 1, 61108 Харьков, Украина*

В этой роботе исследовались физические и механические свойства сплава Zr1 % Nb облучённого с помощью пучка ионов Kr с энергией 107 МэВ, флюэнсами $1{\cdot}10^{13}$ и 10^{14} ион/см^2, а также под влиянием микросекундного сильноточного импульсного пучка электронов с энергий 370 кэВ, падающим потоком энергии в интервале 20…200 Дж/см^2. Низкоинтенсивная имплантация ионов Kr вызвала размягчение сплава. Высокоинтенсивное облучение ионным пучком привело к образованию поверхностного упрочненного слоя с нанотвёрдостью 4.5 ГПа и модулем упругости 120 ГПа. Облучение сильноточным электронным пучком вызвало макроскопическое поверхностное оплавление образца, что привело к образованию крупнозернистой структуры с преимущественно хрупким характером излома.

Ключевые слова: Цирконий, Электронный пучок, Быстрые тяжелые ионы, Абляция.

REFERENCES

1. S Brinton, www.thirdway.org/report/the-advanced-nuclear-industry.
2. *Thermophysical Properties of Materials For Nuclear Engineering: a Tutorial and Collection of Data*, 191 (IAEA: Vienna: 2008).
3. A.M. Dovbnya, S.D. Lavrinenko, V.V. Zackutin, et al, *Probl. At. Sci. Tech.* **72** No 2, 39 (2011).
4. Н.Н. Рыкалин, И.В. Зуев, А.А. Углов, *Основы электронно-лучевой обработки материалов*, 239 (Москва: Машиностроение: 1978) (N.N. Rykalin, I.V. Zuyev, A.A. Uglov, *Osnovy elektronno-luchevoy obrabotki materialov,* 239 (Moskva: Mashinostroyeniye: 1978)) [in Russian].
5. B.A. Kalin, N.V. Volkov, E.A. Anan'eva, *J. Surf. Invest.* **4** No 3, 538 (2010).
6. D.K. Avasthi, G.K. Mehta, *Swift Heavy Ions for Materials Engineering and Nanostructuring*, 280 (Springer Series in Material Science 145: 2011).
7. C. Yan, R. Wang et al, *J. Nucl. Mater.* **461**, 78 (2015).
8. A. Benyagoub, F. Levesque, et al, *App. Phys. Lett.* **77**, 3197 (2000).
9. Н.С. Пушилина, *Исследование модификации поверхности циркониевого сплава импульсным электронным пучком* (Томск: 2011) (N.S. Pushilina, *Issledovaniye modifikatsii poverkhnosti tsirkoniyevogo splava impul'snym elektronnym puchkom* (Tomsk: 2011)) [in Russian].
10. Г.С. Романов, М.В. Сузденков, *Доклады Академии наук БССР* **XXVI** No 6 (1982) (G.S. Romanov, M.V. Suzdenkov, *Doklady Akademii nauk BSSR XXVI* No 6 (1982)) [in Russian].
11. А.Е. Майер, *Динамические процессы и структурные превращения в металлах при облучении интенсивными потоками заряженных частиц*, 34 (Челябинск: 2011) (A.Ye. Mayyer, *Dinamicheskiye protsessy i strukturnyye prevrashcheniya v metallakh pri obluchenii intensivnymi potokami zaryazhennykh chastits,* 34 (Chelyabinsk: 2011)) [in Russian].
12. Yu.F. Lonin, I.J. Magda, *Probl. At. Sci. Tech.* **57** No 5, 85 (2008).
13. A.G. Kobets, P.R. Horodek et al., *Surf. Eng. Appl. Electrochem.* **51** No 5, 478 (2015).
14. V.F. Klepikov, Yu.F. Lonin et al, *Probl. At. Sci. Tech.* **96** No 2, 39 (2015).
15. S.E. Donets, V.F. Klepikov et al, *Probl. At. Sci. Tech.* **98** No 4, 302 (2015).
16. B. Gikal, S. Dmitriev et al, *18th International Conference – Cyclotrons 2007,* 27 (Giardini Naxos: 2007).
17. G.S. Was, *Fundamentals of Radiation Materials Science. Metals and Alloys*, 839 (Springer-Verlag: Berlin Heidelberg: 2007).
F. Onimus, J.L. Bechade, *Comprehensive Nuclear Mater.* **4.01**, 221 (2012).